ISSN 0001-4338, Izvestiya, Atmospheric and Oceanic Physics, 2024, Vol. 60, No. 6, pp. 689–698. © Pleiades Publishing, Ltd., 2024.

Determining the Total Ozone Column from Spectral Measurements of IKFS-2 in 2015–2022

A. V. Polyakov[a, *], E. P. Kriukovskikh[a, **], Ya. A. Virolainen[a, *], G. M. Nerobelov[a, b, c, ****], D. A. Kozlov[d, *****], and Yu. M. Timofeyev[a, ******]**

[a] *St. Petersburg University, St Petersburg, 199034 Russia*

[b] *Scientific Research Centre for Ecological Safety, Russian Academy of Sciences, St Petersburg, 187110 Russia*

[c] *Russian State Hydrometeorological University, St. Petersburg, 195196 Russia*

[d] *Keldysh Research Center, Moscow, 125438 Russia*

**e-mail: a.v.polyakov@spbu.ru*

***e-mail: kriukovskikh1967@mail.ru*

****e-mail: yana.virolainen@spbu.ru*

*****e-mail: akulishe95@mail.ru*

******e-mail: dakozlov@kerc.msk.ru*

*******e-mail: y.timofeev@spbu.ru*

Received May 28, 2024; revised August 14, 2024; accepted September 2, 2024

Abstract—The results of determining the ozone total column (OTC) from the spectra of the outgoing thermal infrared radiation measured by the IKFS-2 instrument from the Meteor-M No. 2 spacecraft during 8 years of measurements are presented. The previously developed technique for the interpretation of spectral measurements made in 2015–2020 with a swath width (SW) of 1000 km is applied to the measurements in 2021–2022 with a SW of 1500 km. It is shown that the increase in the differences between the IKFS-2 data and the results of independent measurements is caused not by the expansion of the OTC variability statistics, but by the increase in the range of scanning angle variation. After a finalization of the technique for the measurements with a 1500-km SW, a comparison with independent data showed that the standard deviations of differences with the results of ground and satellite measurements for all 8 years do not exceed 3% and did not increase compared to the first 6 years of measurements. To analyze the results in the polar regions, the OTC values obtained from the IKFS-2 spectra are compared with the ozonesonde data, which are performed continuously throughout the year, including the polar night. A good qualitative agreement of the IKFS-2 data and ozone sounding data, including winter–spring periods of extreme OTC decrease at high latitudes of both hemispheres, is shown. The standard deviations of the differences between the IKFS-2 data and the OTC values from ozone sounding data were from 5.3 to 11% (17–33 DU) for different stations, or on average for all stations 7.9%, which is consistent with the uncertainty of the estimates of the integrated ozone content in the vertical column from ozonesonde data.

Keywords: remote sensing of the atmosphere, atmospheric ozone, IKFS-2, ozone total column

DOI: 10.1134/S0001433824700713

1. INTRODUCTION

Ozone is one of the most important gases in the Earth's atmosphere. Despite its low concentrations in the atmosphere, ozone in the stratosphere is vital for the biosphere, as it protects flora and fauna (including humans) from harmful ultraviolet (UV) radiation from the Sun (WMO, 2022). At the same time, ozone, which is found in the ground layer of the atmosphere, is included in the list of five most important atmospheric pollutants that affect public health. In addition, at the upper boundary of the troposphere, ozone makes a significant contribution to the greenhouse effect: from 7 to 22% (WHO, 2021).

Atmospheric ozone has attracted attention since the discovery in the 1980s of a significant decrease in its stratospheric content, up to the formation of "ozone holes," caused by anthropogenic factors (WMO, 2022), which led to the development of various systems for monitoring changes in atmospheric ozone. Although the atmospheric levels of ozone-depleting gases have been decreasing since the adoption of a number of international agreements to limit and ban them, they are still present in the atmosphere, and in recent years there have been variations in the rate of their decrease, caused by both natural and anthropogenic factors (WMO, 2022). The expected

recovery of the ozone layer thickness to pre-1980 values is gradually being pushed back to the end of the 21st century, while, due to the growth of greenhouse gas emissions, the prospects for changes in the ozone total column (OTC) on a global scale are still unclear (WMO 2022, 2023). Thus, ozone monitoring remains a pressing issue, especially in polar regions, where, on the one hand, there is a significantly different variability in the seasonal decrease in ozone content from year to year, and, on the other hand, during the polar night and when the Sun is low, it is difficult to use the most widely used methods of ozone observation based on measurements of solar radiation.

Various methods, both contact and remote, are used to monitor atmospheric ozone content. Contact methods are characterized by higher accuracy and better temporal resolution (e.g., Andreev et al. (2023)), while remote sensing methods, especially satellite methods, provide global spatial coverage and continuity of measurements. Examples of satellite ozonometric instruments include the Tropospheric Monitoring Instrument (TROPOMI) on board the Sentinel5P satellite (Veefkind et al., 2012) and the Ozone Monitoring Instrument (OMI) on the Aura satellite (McPeters et al., 2008, 2015). In addition to satellites, remote sensing methods are also widely used at ground-based observation stations. Common ground-based remote sensing methods use solar radiation in the UV, visible, and infrared (IR) spectral ranges. Methods for measuring direct and scattered solar radiation transmitted through the atmosphere using Dobson and Brewer instruments, the Russian M-124 ozonometer, and IR Fourier spectrometers are widely used to validate satellite methods, both when launching new instruments and throughout their operation, in particular to determine drift in time series of data.

Satellite methods for ozone monitoring can be divided into three main types: (1) based on reflected and scattered solar radiation (for examples OMI and TROPOMI); (2) limb methods—transparency, using radiation from the Sun: the Atmospheric Chemistry Experiment–Fourier Transform Spectrometer (ACE-FTS) (Bernath et al., 2017) or other natural radiation sources (for example, stars: Global Ozone Monitoring by Occultation of Stars (GOMOS) (Bertaux et al., 1991)), as well as the atmosphere's own radiation in the microwave (Microwave Limb Sounder (MLS) (Lee et al., 2005)) or IR (Michelson Interferometer for Passive Atmospheric Sounding (MIPAS) (Glatthor et al., 2006)) spectral regions; and, finally, (3) nadir methods using thermal IR radiation from the atmosphere and surface (Infrared Atmospheric Sounding Interferometer (IASI) (Boynard et al., 2016), Infrared Fourier Spectrometer (IKFS)-2 (Polyakov et al., 2023), etc.).

With limb measurements, information about the gas composition of the atmosphere can be obtained with the exception of the lower layers (no higher than 5–7 km); i.e., these methods do not allow one to obtain information about the total gas content in a vertical column. In addition, limb measurements do not allow one to obtain data with satisfactory horizontal resolution and measurement localization. At the same time, only methods based on measuring the outgoing thermal radiation of the atmosphere and surface, for example, based on spectral measurements of the Russian IKFS-2 instrument, allow one to obtain information about OTC with a wide coverage in the polar regions during and around the polar night.

Previously, an analysis of IKFS-2 OTC measurements together with an analysis of ERA5 reanalysis data on temperature and potential vorticity allowed a detailed study of the evolution of the polar stratospheric vortex and ozone miniholes in the Northern Hemisphere in March and April 2020 (Polyakov et al., 2021). OTC measurements for 2015–2020 (Polyakov et al., 2023) were used to analyze ozone distribution fields in the Arctic and Antarctic in the winter–spring in different years.

In this paper, we consider the application of the OTC determination technique from outgoing thermal IR spectra that was previously used to process IKFS-2 spectral measurements for 2015–2020 to 2021–2022. As a result, we apply the improved OTC determination methodology to IKFS-2 measurements for 8 years, 2015–2022.

2. METHODOLOGY AND DATA

2.1 Technique for Solving the Inverse Problem and Its Initial Data

The IKFS-2 Fourier spectrometer is designed for installation on Russian Meteor-M meteorological satellites. It measures the outgoing thermal radiation of the surface–atmosphere system in the spectral range of 660–2000 cm^{-1}, with a spectral resolution of 0.7 cm^{-1} in the spectral region we use of 660–1210 cm^{-1}. The error of spectral measurements (Noise-Equivalent Spectral Radiance (NESR)) is estimated during the measurement process and does not exceed values in the range of (0.15–0.45) $mW/(m^2\ cp\ cm^{-1})$ (Golovin et al., 2013). The spectra that were measured are presented on the Planeta Scientific Research Center website (http://planet.rssi.ru/calval/public-ikfs?setlang=ru_RU). In the period up to December 2020, measurements were carried out with a swath-width (SW) of 1000 km. Starting from December 2020, the SW was increased to 1500 km, which made it possible to completely scan the territory of the Russian Federation without gaps for each day of observations. This paper use spectral data obtained over the period from 2015 to the end of 2022.

The method for determining OTC from the spectra of outgoing IR radiation was previously presented in (Garkusha et al., 2017; Polyakov et al., 2021, 2023). It is based on an algorithm for solving the inverse problem of obtaining OTC from spectra measured by the

IKFS-2 Fourier spectrometer on the Russian Meteor-M No. 2 satellite. The algorithm is based on the use of artificial neural networks (ANN), the principal component (PC) method, and OTC measurement data from the OMI satellite instrument. The error in determining OTC is less than 3%; the method allows for the analysis of the global distribution of OTC, including during polar nights.

The algorithm for solving the inverse problem uses the simplest type of ANN—a three-layer perceptron (see, for example, (Wasserman, 1992)), the input parameters of which (predictors) are the zenith angle of the satellite when observed from the measured pixel, the fraction of the year (the ratio of the day number of the year to the length of the year), and latitude and PC of the IKFS-2 spectrum. Details of the algorithm for solving the inverse problem are given in (Polyakov et al., 2021, 2023). Based on the estimates of the paper (Garkusha et al., 2017), 25 PCs of the spectrum section 660–1210 cm^{-1} are used, containing information on the vertical distribution of temperature, humidity, and surface properties, as well as a 50 PC section of the spectrum containing only the ozone absorption band, namely, 980–1080 cm^{-1}. A similar approach has been previously used by other researchers, for example in (Turquety, et al., 2004; Clerbaux et al., 2009) for the IASI instrument. The main difference of our work is the use of the widest possible ensemble of data for training. For this purpose, a set of pairs of IKFS-2 spectral measurements and OTC level 2 data were created, i.e., single measurements obtained by the OMI instrument (McPeters, et al., 2008, 2015). The instrument takes measurements onboard the Aura satellite with a spatial resolution of 13 × 24 km, scanning a 2500 km wide strip across the direction of the satellite's movement (McPeters, et al., 2008, 2015; Kuttippurath, et al., 2018). The OMI instrument measures scattered solar radiation in the wavelength range of 270–500 nm with a spectral resolution of about 0.5 nm, and the OTC value is measured with an error of 1–2% (McPeters, et al., 2008, 2015). It is also important that OMI measurements provide global coverage of the Earth's surface. Using extensively validated data to train ANNs made it possible to remove the issue of calibration of the results obtained from IKFS-2 data. OMI instrument data version 3, were obtained from (OMI DATA). We use both the original IKFS-2 spectral data processing technique developed for 2015–2020 and its modification to better fit the measurement period after 2020.

2.2 Data for Validation of the Algorithm Application Results

To validate the IKFS-2 OTC measurements, independent OTC data were collected from various sources, including both ground-based ozone network data available on the WOUDC website (WMO/GAW, 2024) and satellite data (TROPOMI instrument). In addition, for the first time, IKFS-2 OTC data are compared with OTC values obtained from ozone sounding.

Data of the ozonometric network is represented by single measurements using Dobson and Brewer instruments. The Dobson spectrometer was developed in 1924 by British physicist and meteorologist Gordon Dobson. The Dobson spectrophotometer can be used to measure both OTC and atmospheric ozone profiles. The spectrometer compares the intensity of solar radiation at two different wavelengths, 305 and 325 nm (in and outside the ozone absorption band), and determines their ratio, which is used to calculate the OTC. The instruments are regularly mutually calibrated, which ensures the consistency of the data (Andreev et al., 2023). The Kipp & Zonen Brewer spectrophotometer, based on similar physical principles, is currently the only automated reference instrument recommended by the World Meteorological Organization (WMO) for measuring total ozone. We only use direct solar radiation measurements, because they are the most accurate. According to (Kerr, 2002), the accuracy of such single measurements is 1–2%.

Ozonesonde data are obtained using specialized sensors installed as an additional unit on conventional meteorological radiosondes and based on the electrochemical principle. These data have a number of significant shortcomings: in particular, ozonesondes very rarely rise above altitudes with a pressure level of 6 hPa, which complicates the calculation of OTC, and the absolute measurement error reaches 10% with a vertical resolution of 100–150 m (GAW, 2014). However, unlike measurements based on solar radiation, ozonesonde data is available throughout the year, including the polar night period. Measurements are taken at different intervals at different stations, but in most cases weekly, on Wednesdays. The format of data supplied by ozonesonde stations includes an estimate of OTC obtained by integrating a synthetic vertical profile collected from ozonesonde measurements and supplemented on top with average climate data. It is noted that such profiles are determined with an accuracy of up to a factor not exceeding 0.1 in absolute value. If synchronous optical measurements of OTC are available with Dobson or Brewer instruments, they are calibrated against the latest (WMO, 2021). Although such a calibration cannot be performed during the polar night period, ozonesonde data are the only source of OTC information based on physical principles different from those used in our approach, which is essential for validation.

TROPOMI began OTC measurements from Sentinel 5 Precursor (S5P) (Veefkind, et al., 2012) in May 2018, with a spatial resolution of 3.5 × 7 km (Garane et al., 2019) and, later, 3.5 × 5.5 km (TROPOMI DATA). In the paper (Garane et al., 2019), OTC data from TROPOMI were compared with ground-based measurements by Brewer, Dobson, and Differential

Table 1. Results of a comparison of OTC data from IKFS-2 with data from satellite (TROPOMI) and ground-based (Dobson, Brewer instruments) measurements. Mean differences (MD) and standard deviation (SD) of the difference in measurements

1	2	3	4		5	
No.	ANN training period (scan width)	Comparison period (scan width)	Satellite measurements		Ground measurements	
			MD, %	SD, %	MD, %	SD, %
1	2015–2020 (1000)	2015–2020 (1000)	–2.14	2.71	–0.47	2.73
2		2015–2022 (1500)	–2.04	3.00	–0.22	2.83
3		2021–2022 (1500)	–1.91	3.29	0.14	2.94
4		2021–2022 (1000)	–2.61	2.88	0.89	2.52
5		2021–2022(1000–1500)	–0.57	3.60	–.02	3.0
6	2015–2022 (1500)	2015–2022 (1500)	–2.22	2.73	–0.41	2.67
7		2021–2022 (1500)	–2.36	2.82	–0.80	2.35
8		2021–2022 (1000)	–2.52	2.77	0.21	2.28
9		2021–2022(1000–1500)	–2.05	2.88	–1.02	2.30
10		2015–2020 (1000)	–2.09	2.64	–0.40	2.71

Optical Absorption Spectroscopy (DOAS) instruments, with mean differences (MDs) ranging from 0 to 1.5% and standard deviations of differences (SD) from 2.5 to 4.5%. For comparison with OTC IKFS-2 data, we used TROPOMI level 2 measurements (TROPOMI DATA), filtered by quality flag (greater than 0.9). The data used were RPRO (reprocessed, the final processed version of the data) (before August 26, 2022) and OFFL (offline, the first version of the data obtained after receiving the spectral measurements) after the specified date; i.e., the results of the highest quality data processing available at the time data were received from the Internet on March 5, 2024. Due to the peculiarities of the orbits of the Meteor-M No. 2 and Sentinel 5P satellites, we used data with a time mismatch of up to 6 h. Smaller mismatches limit data availability in tropical and midlatitudes. To exclude unreliable near-zero and absurdly high OTC values, we looked at TROPOMI data in the range of 100–650 for comparison.

3. Results of Applying the Technique for the Period 2021–2022

In the first stage of our study, we applied technique developed based on the 2015–2020 data to process the 2021–2022 spectra without any modifications. We compared the OTC values with data from the TROPOMI instrument and data from the WOUDC ground-based ozonometric network (WMO/GAW, 2024). In Table 1, we present the mean and root-mean-square differences between IKFS-2 data and data obtained from independent sources, showing also the results of similar comparisons for 2015–2020 and 2015–2022. Here and everywhere below, we used the following criteria for the consistency of data pairs: IKFS-2 and ground-based instrument measurements within 1 h in time and within 70 km in distance from the center of the sounding pixel to the ground-based instrument and IKFS-2 and TROPOMI measurements within 6 h in time and within 35 km in distance of pixel centers from each other. The choice of parameters for the permissible mismatch and the list of 21 stations that provided individual OTC measurement data, with which the comparison was performed, are substantiated in (Polyakov et al., 2021, 2023). The list and location of stations are presented in the first few columns of Table 2. As can be seen from Table 2, the ozonometric stations we use are located mainly in the middle latitudes of the Northern Hemisphere in Europe and the United States. However, two stations are located north of the Arctic Circle, four are in the tropical zone, and two are in the Southern Hemisphere. The last three columns of Table 2 will be analyzed below.

Let us return to Table 1. Row 1 of Table 1 is actually a repetition of the results presented in (Polyakov et al., 2023), but using updated and supplemented independent data for comparisons. Note that the values given in row 1 of Table 1 differ slightly from the results of (Polyakov et al., 2023), which obtained SD values of 2.9% for single ground-based and 2.75% for satellite measurements. Changes in ground data are due to their replenishment: data from measuring stations are gradually received by the WOUDC website over several years after measurements. The TROPOMI data update is due to the difference between the final RPRO and preliminary OFFL versions of the instrument's spectral measurement processing—these versions of RPRO.

Table 2. Differences between IKFS-2 and ground-based OTC (WOUDC) data relative to ground-based measurements; spatial and temporal discrepancies are 70 km and 1 h; instrument type (Brewer (B) or Dobson (D)) is in column I. ANN trained on 8 years of data; statistics for 8 years

No.	I	Station name	Latitude, degrees	Longitude, degrees	Height, m	Number of comparisons	MD, %	SD, %
1	B	Eureka	80.05	−86.42	9	162224	−0.4	2.5
2	B	Resolute	74.70	−94.97	68	73496	−0.8	2.3
3	B	Churchill	58.75	−94.07	26	15630	−1.5	2.5
4	B	Obninsk	55.10	36.610	100	972	−0.1	3.0
5	B	Edmonton	53.55	−114.11	752	20089	0.7	3.0
6	B	Goose Bay	53.31	−60.36	26	17773	−0.2	2.2
7	B	Lindenberg	52.21	14.12	127	12778	−1.5	2.8
8	B	De Bilt	52.10	5.18	24	13801	−2.7	2.1
9	D	Kyiv-Goloseyev	50.36	30.50	206	3780	−0.2	2.0
10	B	Saturna Island	48.77	−123.13	202	17458	−0.1	2.2
11	B	Aosta	45.74	7.36	570	1736	0.6	1.7
12	B	Egbert	44.23	−79.78	264	12256	−1.4	2.0
13	D	Lannemezan	44.13	0.37	590	118	2.0	1.8
14	B	Toronto	43.78	−79.47	202	56548	−1.0	2.2
15	B	Kislovodsk	43.73	42.66	2070	3768	1.6	2.4
16	B	Thessaloniki	40.63	22.96	60	8121	−1.2	2.2
17	D	Univ. of Tehran	35.73	51.38	1419	852	1.0	2.1
18	B	Mauna Loa (HI)	19.54	−155.58	3397	32487	2.2	3.5
19	B	Paramaribo	5.81	−55.21	16	11571	−0.4	2.1
20	D	Natal	−5.84	−35.21	49	32	0.9	1.2
21	D	Cachoeira-Paulista	−22.69	−46.20	574	24	−3.1	1.8
		All stations				469158	−0.4	2.7

From row 2 of Table 1, we can see that, when adding measurements from the last 2 years, MDs decreased slightly and SDs increased for both types of comparisons. The reasons for the increase may be both (a) the expansion of the scanning band and (b) the inadequacy of the ozone variability statistics for 6 years and for 2021–2022. From lines 3–5, it is clear that a comparison of all data for the last 2 years of measurements leads to an increase in SD for ground-based measurements to 2.94%, and for satellite measurements to 3.29% (line 3), while a comparison for the same period with only data within a 1000-km-wide band for these 2 years (line 4) reduces the SD for ground-based measurements and slightly increases it for satellite measurements. Selecting measurements with SW between 1000 and 1500 km (line 5) shows a significant increase in SD: 3.0% for terrestrial data and up to 3.6% for satellite data. From this we can conclude that the increase in SD is caused mainly by the expansion of the scanning band.

Rows 6–10 of Table 1 show the results of comparisons that replicate rows 1–5, but for an ANN trained on the full data set. An analysis of this part of Table 1 shows that the "new" ANN allows for the entire 8-year measurement period to obtain discrepancies no worse than for the first 6 years, without worsening the results for the first 6 years relative to the "old" ANN. It should be noted that the values of the standard deviations of the differences remain quite close to each other for different measurement periods and scanning bandwidths.

Thus, the analysis of Table 1 allows us to conclude that the OTC variability for the first 6 years of measurements represents a data ensemble that is sufficiently wide and adequate for estimating OTC from spectral measurements in the following 2 years.

4. Discussion: Comparison with Data from Individual Ozone Stations and Ozone Sounding Data

The last three columns of Table 2 present the results of a comparison of IKFS-2 data with ground-based ozonometric station data over 8 years. As can be seen, the average OTC differences between satellite and ground-based data range from −3.1 to 2.2%. Such variability may be associated with both different cali-

brations of ground-based equipment and different surface topography near ozonometric stations. In particular, the largest positive difference (i.e., the excess of IKFS-2 data over ground-based measurements) corresponds to measurements at the Mauna Loa station (row 18), located on the top of a mountain on an island at an altitude of 3307 m. Data from this station are compared with IKFS-2 measurements with a spatial resolution of 35 km at nadir, sampled in a circle with a radius of 70 km, i.e., mostly above the ocean surface. This difference is sufficient to produce a noticeable systematic difference. The maximum negative difference of –3.5% for the Cachoeira-Paulista station (line 21) is not statistically significant, since it was obtained on the basis of only 24 measurements. However, the next largest difference for the De Bilt station (line 8) cannot be related to the topography of the area and is probably explained by the calibration of the ground-based instrument. The maximum standard deviation of the difference (last column) also corresponds to the Mauna Loa station (row 18) and is caused, according to our assumptions, by the heterogeneity of the surface—partly mountainous terrain, partly the ocean surface, which results in different atmospheric thicknesses and, accordingly, OTC variability. All other SD values are less than 3%. Taking into account the presence of errors in the ground-based measurement data, it can be concluded that the measurement error of IKFS-2 does not exceed 3% for measurements near all the ozonometric stations considered.

As was noted above, during the polar night, measurements of solar radiation by TROPOMI, OMI, and similar satellite instruments, as well as by ground-based instruments, are impossible. Apart from IR sounders like IKFS-2, the only source of OTC data during this period in the polar regions is ozonesondes data. Let us analyze how the results of OTC calculations using our technique relate to this data. We used ozonesonde data harmonized by the HEGIFTOM working group within the TOAR-II project (HEGIFTOM database). The database of this project, at the time of our access to it on February 20, 2024, contained data on 57 ozone sounding stations in varying degrees of preparation (harmonization). In fact, 40 stations were ready for use.

For comparison, IKFS-2 measurements were selected in a circle centered on the coordinates of the ozone sounding station and with a radius of 70 km and a measurement time mismatch of 1 h. Due to the peculiarities of the satellite's trajectory, a circle with a radius of about 150 km around the South Pole is inaccessible for measurements even for a SW of 1500 km. Therefore, for comparisons with data from this station, IKFS-2 data were used in a circle with a radius of 200 km, but even so, comparisons are only possible starting from December 2020.

As mentioned earlier, the OTC at ozonesonde stations was calculated using ozonesonde profiles supplemented with average climate data (WMO, 2021). Since the maximum altitude reached by the probe is random and limited by the balloon rupture, the upper limit of the measured profile (ULMP) varies over a wide range of atmospheric pressure levels, from units to several hundred hectopascals. Obviously, the accuracy of calculating the OTC improves as the maximum ULMP (minimum pressure) is reached. Therefore, we used only those measurements in which the ULMP was above the 10 hPa pressure level. Station data is supplied in various formats. Ten of the stations we examined use a format that presents the integral ozone content in a vertical column only up to the ULMP. The remaining stations provide OTC calculated from ozonesonde data supplemented with average climate data. We used both types of data for comparison because, despite the larger absolute value of MD, the SD values for the first type of data show satisfactory agreement with the OTC values from IKFS-2 measurements. Since the amount of data from such stations is small, their contribution to the growth of the total MD value also turned out to be insignificant.

The SD of the IKFS-2 data and the OTC values from ozone sounding data ranged from 5.3 to 11% (17–33 DU) for different stations; the MD and SD values averaged over all stations were 1.2 and 7.9%, which is consistent with the uncertainty of the integral ozone content in the vertical column from ozone sounding data.

For a qualitative comparison in the form of a graphical presentation, we selected stations that provide OTC data and for which both the number of measurements for 2015–2022 and the number of ozonesonde–IKFS-2 measurement pairs exceed 100. To provide a more detailed picture of ozone variability, we show not paired measurement results but the OTC values for IKFS-2 averaged over a day in a circle centered on the station location. The radius of this circle for the South Pole station is 500 km, and for other stations it is 70 km. Such a large circle size for the South Pole station was chosen to allow the analysis of measurements with SW 1000 km, which, due to the specifics of the satellite orbit, cannot be obtained closer than 400 km to the South Pole. The sufficiently high homogeneity of the surface and atmosphere in this region made it possible to use for comparisons the actual average value in a ring 100 km wide with an inner radius of 400 km. For ozone sounding data, single measurements are shown.

Such qualitative comparisons were performed for stations for which (a) OTC data were provided and (b) measurements were available in sufficient quantity during the IKFS-2 operation period of 2015–2022. There are 13 such ozone sounding stations in the HEGIFTOM database; they are located in all latitudinal zones. The comparisons showed good agreement between the results of the two types of measurements, both in terms of the magnitude of the spread of values and in the OTC values themselves.

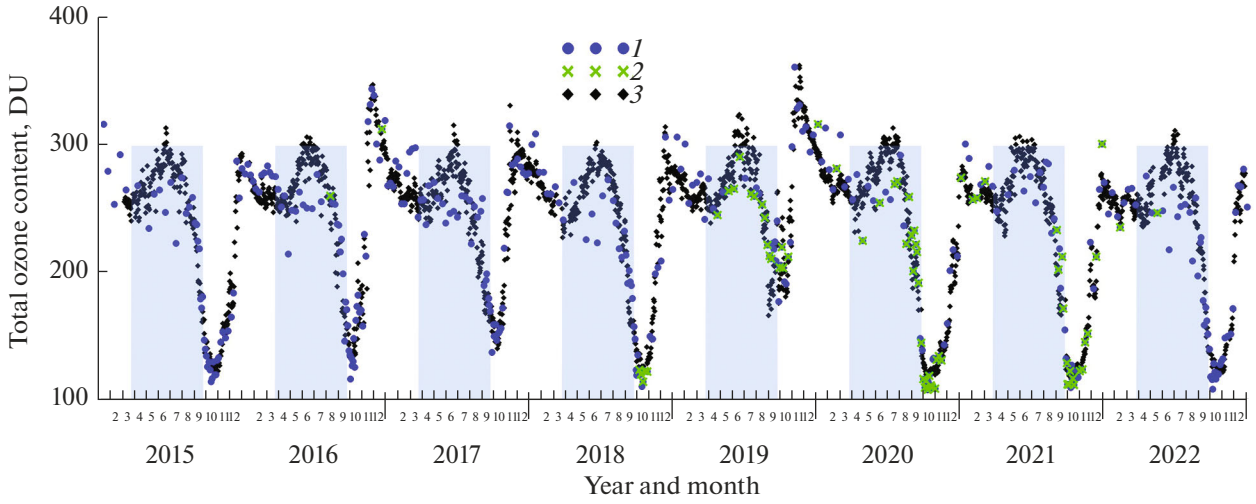

Fig. 1. OTC based on ozone sounding data from the South Pole station and average daily OTC from IKFS-2 in a circle with a radius of 500 km. The periods of polar night are highlighted in color. (*1*) All ozonesondes; (*2*) ozonesondes that reached the level of 10 hPa; and (*3*) IKFS-2, daily average in a circle with a radius of 500 km.

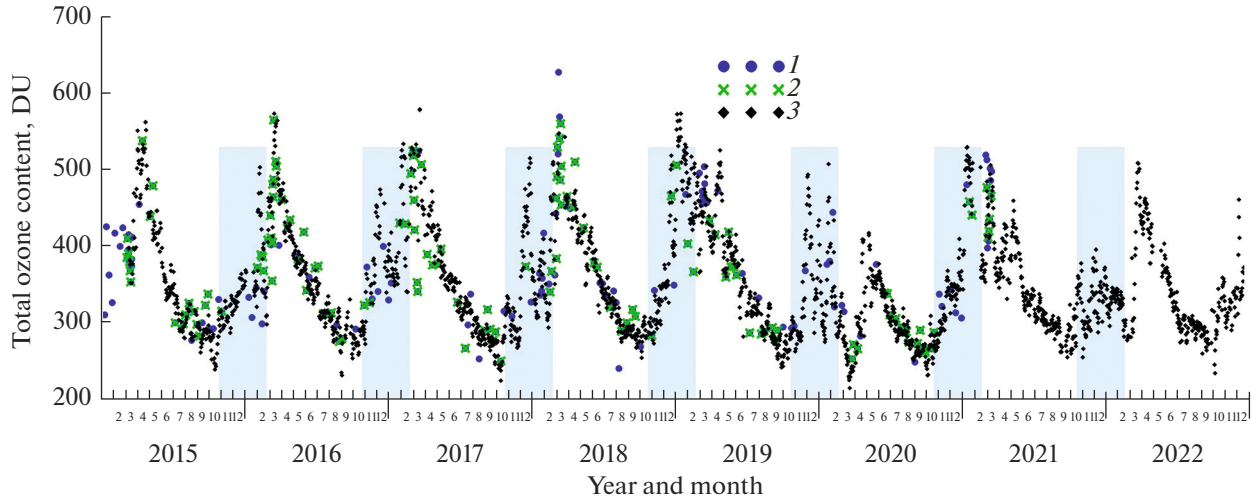

Fig. 2. OTC based on ozone sounding data from the Eureka station (80° N) and average daily OTC from IKFS-2 in a circle with a radius of 70 km. The periods of polar night are highlighted in color. (*1*) All ozonesondes; (*2*) ozonesondes that reached the level of 10 hPa; and (*3*) IKFS-2, daily average in a circle with a radius of 70 km.

As an example, Fig. 1–3 show OTC values based on radiosonde and IKFS-2 data in the region of both poles and near the tropical zone. As was mentioned above, only a portion of ozonesondes rise to the 10 hPa level, which is apparently determined primarily by the quality of the cylinder. Obviously, the higher the ozonesonde rises, the more accurately the OTC can be calculated based on its measurement data. Therefore, we selected the data obtained when the probe rose above the 10 hPa level.

Figure 1 shows that in the South Pole region there is good qualitative agreement between the IKFS-2 data and the ozonesonde data: high OTC values are observed in the December–July period, which are also accompanied by a relatively large (and mutually close) variability in both the IKFS-2 and the sounding data. At the same time, random differences between them are large, which is due to the large variability of OTC values. At the same time, during the period of decreasing OTC from July to November, its variability, although increasing, is of a systematic nature (decline and then growth), and the IKFS-2 and ozonesonde data are in good mutual agreement. Let us note one peculiarity: a less significant decrease in OTC in the spring of 2019 than in other years, recorded by both types of measurements. Thus, the IKFS-2 OTC in the South Pole region is in good qualitative agreement with ozonesonde data.

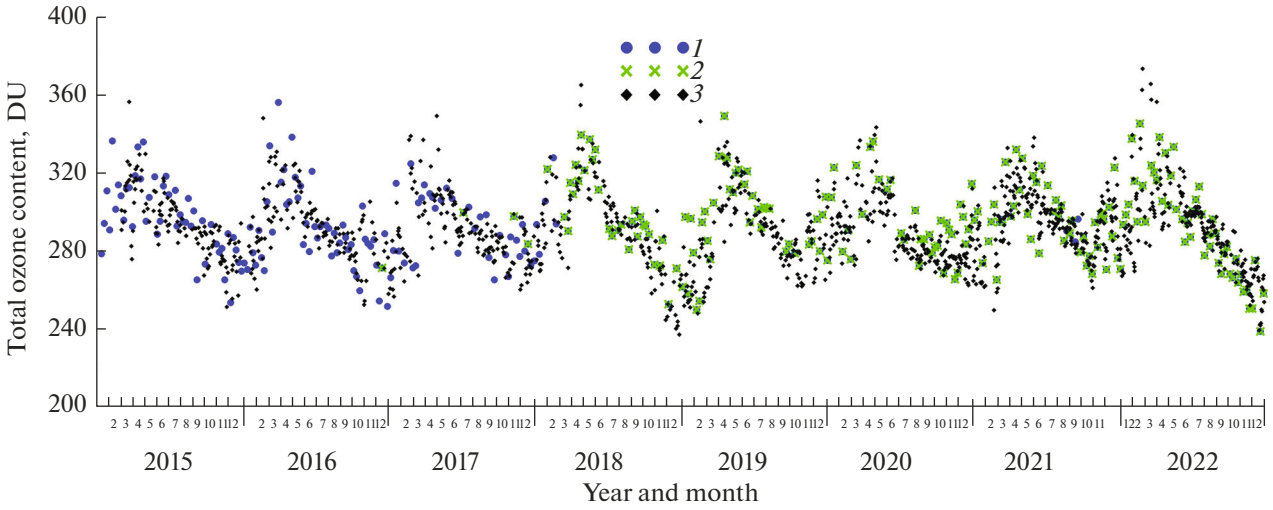

Fig. 3 OTC based on ozone sounding data from the Tenerife station (28° N) and average daily OTC from IKFS-2 in a circle with a radius of 70 km. (*1*) All ozonesondes; (*2*) ozonesondes that reached the level of 10 hPa; and (*3*) IKFS-2, daily average in a circle with a radius of 70 km.

Figure 2 shows similar comparisons for the Eureka observing station located at 80° N. Here, apparently for some technical reasons, during the polar night, the number of probes that reach the 10 hPa level sharply decreases. At the same time, during the same period, an increase in random variability of OTC is observed according to data from both types of measurements, but the trend of OTC growth consistently persists throughout the polar night. It should be noted that extremely high OTC values in March for a number of years are consistently observed according to data from both types of measurements. The subsequent spring–summer decrease in OTC is also observed consistently for both types of measurements. We conclude that, at high latitudes of the Northern Hemisphere, good qualitative agreement between the two types of measurements is also observed.

Figure 3, which shows a comparison for a station on the island of Tenerife, also shows good agreement both in the variability of the OTC value and in its seasonal course.

CONCLUSIONS

1. Using an ANN trained on November 2015–2020 data with a 1000-km SW to derive OTC from IKFS-2 spectral measurements in the period December 2020–2022 with a 1500-km SW shows an increase in the mismatch from 2.7 to 3 and 3.3% when compared with independent ground-based and satellite measurements, respectively.

2. The increase is primarily due to the expansion of the scanning band, rather than to inadequacy of ozone variability statistics in 2015–2020 and 2021–2022.

3. After retraining the ANN, the disagreement with independent measurement data both for the last 2 years and for the entire IKFS-2 measurement period did not worsen compared to December 2015–2020, which gives an estimate of the IKFS-2 data error not exceeding 3%.

4. A comparison of the OTC variability based on IKFS-2 data with ozone sounding data showed good qualitative agreement between the data obtained from two independent sources, including during the polar night.

5. A quantitative comparison of IKFS-2 results with ozone sounding data also demonstrated their good agreement: average differences were 1.2%, and standard deviations of differences were 7.9%, which corresponds to the errors in OTC measurement using ozone sounding data.

ACKNOWLEDGMENTS

We thank the GES DISC Data and Information Service Center for providing access to TROPOMI and OMI data, the Planeta Research Center for providing access to the results of IRFS-2 spectral measurements, and the HEGIFTOM working group within the TOAR-II project for providing access to harmonized ozonesonde measurement data.

To determine the time of the polar night, we used an online calculator for the beginning and end of the day (https://planetcalc.ru/300).

FUNDING

This work was carried out with support from St. Petersburg State University, project code 116234986.

CONFLICT OF INTEREST

The authors of this work declare that they have no conflicts of interest.

REFERENCES

Andreev, V.V., Bazhenov, O.E., Belan, B.D., Vargin, P.N., Gruzdev, A.N., Elansky, N.F., Zhamsueva, G.S., Zayakhanov, A.S., Kotel'nikov, S.N., Kuznetsova, I.N., Kulikov, M.Yu., Nevzorov, A.V., Obolkin, V.A., Postylyakov, O.V., Rozanov, E.V., et al., Russian Studies of Atmospheric Ozone and Its Precursors in 2019–2022, *Izv., Atmos. Ocean. Phys.*, 2023, vol. 59, no. S3, pp. S437–S461. https://doi.org/10.1134/S0001433823150021

Bernath, P.F., The Atmospheric Chemistry Experiment (ACE), *J. Quant. Spectrosc. Radiat. Transfer*, 2017, vol. 186, pp. 3–16.

Bertaux, J.L., Megie, G., Widemann, T., Chassefiere, E., Pellinen, R., Kyrola, E., Korpela, S., and Simon, P., Monitoring of ozone trend by stellar occultations: The GOMOS instrument, *Adv. Space Res.*, 1991, vol. 11, no. 3, pp. 237–242. https://doi.org/10.1016/0273-1177(91)90426-K

Boynard, A., Hurtmans, D., Koukouli, M.E., Goutail, F., Bureau, J., Safieddine, S., Lerot, C., Hadji-Lazaro, J., Wespes, C., and Pommereau, J.-P., Seven years of IASI ozone retrievals from FORLI: Validation with independent total column and vertical profile measurements, *Atmos. Meas. Tech.*, 2016, vol. 9, pp. 4327–4353.

Clerbaux, C., Boynard, A., Clarisse, L., George, M., Hadji-Lazaro, J., Herbin, H., Hurtmans, D., Pommier, M., Razavi, A., Turquety, S., Wespes, C., and Coheur, P.-F., Monitoring of atmospheric composition using the thermal infrared IASI/MetOp sounder, *Atmos. Chem. Phys.*, 2009, vol. 9, pp. 6041–6054. https://doi.org/10.5194/acp-9-6041-2009

Garane, K., Koukouli, M.-E., Verhoelst, T., Lerot, C., Heue, K.-P., Fioletov, V., Balis, D., Bais, A., Bazureau, A., Dehn, A., et al., TROPOMI/S5P total ozone column data: Global ground- based validation and consistency with other satellite missions, *Atmos. Meas. Tech.*, 2019, vol. 12, pp. 5263–5287.

Garkusha, A.S., Polyakov, A.V., Timofeev, Yu.M., and Virolainen, Ya.A., Analysis of capabilities for satellite monitoring of atmospheric gaseous composition using IRFS-2 instrument, *Izv., Atmos. Ocean. Phys.*, 2017, vol. 53, no. 4, pp. 493–501. https://doi.org/10.7868/S0003351517040079

GAW Report no. 201, Quality Assurance and Quality Control for Ozonesonde Measurements in GAW, Geneva: WMO, 2014. https://library.wmo.int/viewer/55131/download?file=gaw_201_en.pdf&type=pdf&navigator=1.

Glatthor, N., von Clarmann, T., Fischer, H., Funke, B., Gil-López, S., Grabowski, U., Höpfner, M., Kellmann, S., Linden, A., López-Puertas, M., Mengistu Tsidu, G., Milz, M., Steck, T., Stiller, G. P., and Wang, D.-Y., Retrieval of stratospheric ozone profiles from MIPAS/ENVISAT limb emission spectra: A sensitivity study, *Atmos. Chem. Phys.*, 2006, vol. 6, no. 10, pp. 2767–2781. https://doi.org/10.5194/acp-6-2767-2006

Golovin, Y.M., Zavelevich, F.S., Nikulin, A.G., Kozlov, D.A., Monakhov, D.O., Kozlov, I.A., Arkhipov, S.A., Tselikov, V.A., Romanovskii, A.S., Spaceborne infrared Fourier-transform spectrometers for temperature and humidity sounding of the Earth's atmosphere, *Izv., Atmos. Ocean. Phys.*, 2014, vol. 50, no. 9, pp. 1004–1015. https://doi.org/10.1134/S0001433814090096

Kerr, J.B., New methodology for deriving total ozone and other atmospheric variables from Brewer spectrophotometer direct sun spectra, *J. Geogr. Res.*, 2002, vol. 107, pp. ACH22-1–ACH22-17.

Kuttippurath, J., Kumar, P., Nair, P.J., and Chakraborty, A., Accuracy of satellite total column zone measurements in polar vortex conditions: Comparison with ground-based observations in 1979–2013, *Remote Sens. Environ.*, 2018, vol. 209, pp. 648–659.

Lee, K.A., Lay, R.R., Jarnot, R.F., Cofield, R.E., Pickett, H.M., Stek, P.C., and Dennis, A., Flower EOS Aura MLS: First year post-launch engineering assessment, *Proc. SPIE*, 2005, p. 58821D. https://doi.org/10.1117/12.620130

Levelt, P.F., Joiner, J., Tamminen, J., Veefkind, J.P., Bhartia, P.K., Zweers, D.C.S., Duncan, B.N., Streets, D.G., Eskes, H., van der A, R., et al., The Ozone Monitoring Instrument: Overview of 14 years in space, *Atmos. Chem. Phys.*, 2018, vol. 18, pp. 5699–5745

McPeters, R.D., Kroon, M., Labow, G., Brinksma, E., Balis, D., Petropavlovskikh, I., Veefkind, J.P., Bhartia, P.K., and Levelt, P.F., Validation of the Aura Ozone Monitoring Instrument total column ozone product, *J. Geophys. Res.*, 2008, vol. 113, p. D15S14.

McPeters, R.D., Frith, S., and Labow, G.J., OMI total column ozone: Extending the long-term data record, *Atmos. Meas. Tech.*, 2015, vol. 8, no. 11, pp. 4845–4850. https://doi.org/10.5194/amt-8-4845-2015

NASA Goddard Space Flight Center Data and Information Services Center. https://disc.gsfc.nasa.gov/. Accessed March 3, 2024.

OMI DATA. https://aura.gesdisc.eosdis.nasa.gov/data/Aura_OMI_Level2/OMTO3.003/. Accessed April 25, 2023.

Polyakov, A., Virolainen, Y., Nerobelov, G., Timofeyev, Y., and Solomatnikova, A., Total ozone measurements using IKFS-2 spectrometer aboard Meteor-M N2 satellite in 2019–2020, *Int. J. Remote Sens.*, 2021, vol. 42, no. 22, pp. 8709–8733. https://doi.org/10.1080/01431161.2021.1985741

Polyakov, A., Virolainen, Y., Nerobelov, G., Kozlov, D., and Timofeyev, Y., Six years of IKFS-2 global ozone total column measurements, *Remote Sens.*, 2023, vol. 15, p. 2481. https://doi.org/10.3390/rs15092481

TOAR-II HEGIFTOM (Harmonization and Evaluation of Ground-based Instruments for Free Tropospheric Ozone Measurements). https://hegiftom.meteo.be/. Accessed February 20, 2024.

TROPOMI DATA Copernicus Sentinel data processed by ESA, German Aerospace Center (DLR), Sentinel-5P TROPOMI Total Ozone Column 1-Orbit L2 5.5km x 3.5km, Greenbelt, Md., Goddard Earth Sciences Data and Information Services Center (GES DISC). March 5, 2024. https://doi.org/10.5270/S5P-fqouvyz

Veefkind, J.P., Aben, I., McMullan, K., Förster, H., De Vries, J., Otter, G., Claas, J., Eskes, H.J.,

De Haan, J.F., and Kleipool, Q., et al., TROPOMI on the ESA Sentinel-5 precursor: A GMES mission for global observations of the atmospheric composition for climate, air quality and ozone layer applications, *Remote Sens. Environ.*, 2012, vol. 120, pp. 70–83.

Wasserman, Ph., *Neural Computing: Theory and Practice*, New York: Van Nostrand, 1989; Moscow: Mir, 1992. WHO global air quality guidelines: Particulate matter (PM2.5 and PM10), ozone, nitrogen dioxide, sulfur dioxide and carbon monoxide, 2021. https://www.who.int/publications/i/item/9789240034228.

WMO/GAW Ozone Monitoring Community, World Meteorological Organization–Global Atmosphere Watch Program (WMO–GAW)/World Ozone and Ultraviolet Radiation Data Centre (WOUDC) Total Ozone Hourly Observations. https://woudc.org. Accessed March 17, 2024.

WMO, Ozonesonde Measurements Principles and Best Operational Practices, GAW Report no. 268, 2021. https://library.wmo.int/records/item/57720-ozonesonde-measurement-principles-and-best-operational-practices.

WMO, Ozone Research and Monitoring, GAW Report no. 278, 2022. https://library.wmo.int/viewer/58360/download?file=2022OzoneAssessment.pdf&type=pdf&navigator=1.

WMO, State of the Global Climate, 2023. https://wmo.int/publication-series/state-of-global-climate-2023.

AI tools may have been used in the translation or editing of this article.